

Subcarriers-To-Subcarriers Beating Interference Cancellation in Radio Frequency-Tone Assisted Baseband Optical Orthogonal Frequency Division Multiplexing System with Symbol Pre-Distortion

Zhaohui Zhang^{1, a}, Yongli Liu^{2, b}, Na Liu^{3, c} and Wenyi Chu^{4, d}

¹State Key Lab of Information Photonics and Optical Communications (Beijing University of Posts and Telecommunications), Beijing 100876, China.

²Quenda Technology Co. LTD, Qingdao 266000, China.

³State Key Lab of Information Photonics and Optical Communications (Beijing University of Posts and Telecommunications), Beijing 100876, China.

⁴Quenda Technology Co. LTD, Qingdao 266000, China.

^azhangzhaohui@bupt.edu.cn, ^bliuyongli@qdsrd.com, ^cluina@bupt.edu.cn, ^dchuwenyi@qdsrd.com

Abstract

Symbol pre-distortion is proposed to restrain subcarriers-to-subcarriers beating interference (SSBI) in radio frequency-tone (RF-tone) assisted baseband optical orthogonal frequency division multiplexing (OFDM) system. Simulation results demonstrate that the 40Gbps 16QAM RF-tone assisted baseband OOFDM system with symbol pre-distortion has a 4dB better sensitivity compared to that without pre-distortion after 100km single mode fiber (SMF) transmission.

Keywords

Symbol pre-distortion, Subcarriers-to-subcarriers beating interference, Direct detection, Orthogonal frequency division multiplexing.

1. INTRODUCTION

Optical OFDM is an attractive candidate for next generation high capacity metro transport networks envisioned to support high speed data rate, multiple services and dynamic bandwidth allocation. The linear impairments, such as chromatic dispersion and polarization mode dispersion, could be compensated by digital signal processing at receiver.

According to the different structure of optical receiver, the optical OFDM can be categorized as Coherent Optical OFDM (CO-OFDM) and Direct Detection Optical OFDM (DD-OFDM). CO-OFDM system possesses better receiving sensitivity but needs high-cost installations, such as narrow line-width laser source and optical hybrid [1], while DD-OFDM requires only photodiodes for detection. DD-OFDM is attractive for short and medium distance beyond 40Gbps data rate transmission due to its receiver simplicity. Double-sideband signal generated by intensity modulator suffers from power fading and subcarriers-to-subcarriers mixing interference (SSMI) after fiber transmission in DD-OFDM [2, 3]. These impairments especially the power fading restrict transmission distance and available signal bandwidth. Single-sideband (SSB) signal generated by IQ modulator or dual-drive Mach-Zehnder modulator (MZM) is impacted by SSBI after direct-detection. The SSBI reduces the available signal bandwidth or

the receiver sensitivity. So a guard band between the optical carrier and the OFDM signal sideband is usually required to avoid SSBI [4]. This guard band reduces the spectral efficiency.

Several techniques have been proposed to eliminate SSBI. Previously reported methods include: (i) subcarrier interleaved: odd-numbered subcarriers carrying data and even-numbered subcarriers adding zeros to make SSBI fall in even-numbered carriers after photodiode. The detection signal is not affected by SSBI at the cost of reducing the spectral efficiency [5]. (ii) Iterated distortion reduction: virtual single-side-band (VSSB) OFDM and iterative detection is used to eliminate the SSBI. To improve system performance, a small gap is reserved, which will also have the problem of lower spectral efficiency [6]. (iii) Compatible single-sideband modulation: the idea is to apply the OFDM signal on the amplitude of the signal [7], and (iv) baseband Optical OFDM: a dual-drive MZM is used to realize SSB modulation with high carrier-to-signal-power ratio (CSPR) and low SSBI [8]. The CSPR in these two methods is higher, generally more than 20dB, so relatively lower signal power is transmitted through fiber which will reduce the receiver sensitivity. (v) Interleaved and turbo-coded OFDM-ROF system: turbo codes and bit interleaver is used to mitigate unbalanced error distribution caused by SSBI. The detrimental impacts are only mitigated but not fundamentally inhibited [9, 10].

In this letter, symbol pre-distortion in baseband optical OFDM system is proposed to restrain SSBI and eliminate the guard band for the first time. To achieve the designed signal after demodulation, the transmitted signal is pre-distorted. The pre-distortion values can be obtained through solving nonlinear equations by fixed point iteration. Most digital signal processing complexity of symbol pre-distortion system is centralized in the transmitter and the low-complexity feature is remained in the receiver. In order to keep the CSPR stable and achieve higher spectral efficiency, the architecture of RF-tone assisted optical carrier and optical carrier suppressed is used [5]. The CSPR can be easily achieved by controlling the relative amplitude of the electrical signal. We show by simulation that the 40Gbps 16QAM optical OFDM system with symbol pre-distortion has a 4dB better receiver sensitivity than that without symbol pre-distortion in 100km metro transport networks.

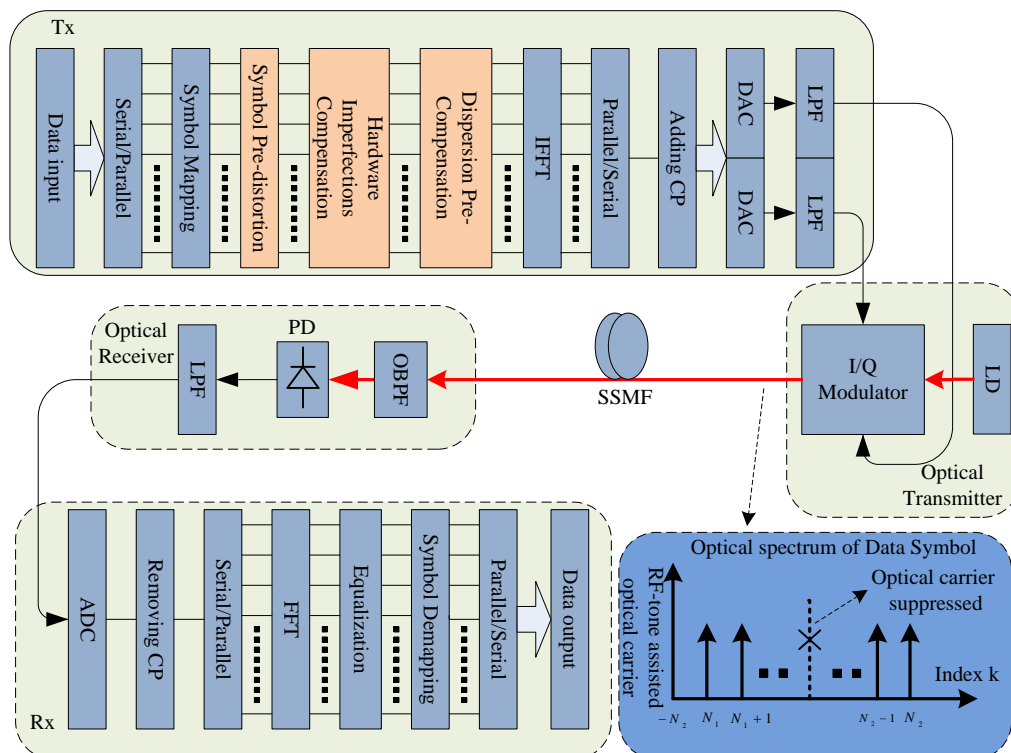


Fig 1. System schematic of RF-tone assisted baseband optical OFDM based on Symbol Pre-distortion. LPF, low-pass filter; OBPF, optical band pass filter; PD, photo-detector

All manuscripts must be in English, also the table and figure texts, otherwise we cannot publish your paper. Please keep a second copy of your manuscript in your office. When receiving the paper, we assume that the corresponding authors grant us the copyright to use the paper for the book or journal in question. Should authors use tables or figures from other Publications, they must ask the corresponding publishers to grant them the right to publish this material in their paper. Use italic for emphasizing a word or phrase. Do not use boldface typing or capital letters except for section headings (cf. remarks on section headings, below).

Do not number your paper: All manuscripts must be in English, also the table and figure texts, otherwise we cannot publish your paper. Please keep a second copy of your manuscript in your office. When receiving the paper, we assume that the corresponding authors grant us the copyright to use the paper for the book or journal in question.

2. ORGANIZATION OF THE TEXT

2.1. Theoretical Models

The principle of symbol pre-distortion scheme is shown in Fig.1 and the mathematical model for symbol pre-distortion is given as follows. The RF-tone assisted discrete-time electrical OFDM signal can be expressed as $E(n) = Ae^{j2\pi(-N_2)n/N} + \sum_{k=N_1}^{N_2} d(k)e^{j2\pi kn/N}$, where A is the assigned amplitude of the RF-tone assisted optical carrier at the $(-N_2)$ -th subcarrier, $d(k)$ is the data symbol modulated on the k -th subcarrier. N_1 and N_2 are the indexes of the left- and rightmost data subcarrier, then $N_2 - N_1 + 1$ is the number of data subcarriers. N is the size of IFFT. If $-N_2 = N_1 - 1$, then there is no guard band. The optical spectrum of data symbol is shown in Fig. 1. Hardware imperfections and fiber chromatic dispersion are pre-compensated at the transmitter. So we assume that there are no hardware imperfections and fiber distortions. After direct detection, the electrical signal infrequency domain can be written as

$$\begin{cases} Y(N_1) = Ad(N_1) + [d(N_1)^* d(N_1 + 1) + d(N_1 + 1)^* d(N_1 + 2) + \dots + d(N_2 - 1)^* d(N_2)] \\ Y(N_1 + 1) = Ad(N_1 + 1) + [d(N_1)^* d(N_1 + 2) + d(N_1 + 1)^* d(N_1 + 3) + \dots + d(N_2 - 2)^* d(N_2)] \\ Y(N_1 + 2) = Ad(N_1 + 2) + [d(N_1)^* d(N_1 + 3) + d(N_1 + 1)^* d(N_1 + 4) + \dots + d(N_2 - 3)^* d(N_2)] \\ \dots \\ Y(N_2 - 1) = Ad(N_2 - 1) + [d(N_1)^* d(N_2)] \\ Y(N_2) = Ad(N_2) \end{cases} \quad (1)$$

Where * represents the complex conjugate and the DC term is disregarded. Received signal $\vec{Y} = [Y(N_1), Y(N_1 + 1), Y(N_1 + 2) \dots Y(N_2 - 1), Y(N_2)]^T$ contains two parts: the first part represents the desired signal, $[Ad(N_1), Ad(N_1 + 1), Ad(N_1 + 2) \dots Ad(N_2 - 1), Ad(N_2)]^T$, and the second part is the SSBI. It's obviously that the SSBI gradually decreases from the leftmost subcarrier, N_1 , to the rightmost subcarrier, N_2 . The N_2 -th subcarrier is not affected by SSBI.

2.2. Principle of Symbol Pre-distortion

From Eq. (1), the demodulated signal \vec{Y} is the sum of the desired signal and the SSBI. Assuming received signal is the desired signal, $\vec{Y} = [Ad(N_1), Ad(N_1 + 1), Ad(N_1 + 2) \dots Ad(N_2 - 1), Ad(N_2)]^T$, and transmitted signal $[d(N_1), d(N_1 + 1), d(N_1 + 2) \dots d(N_2 - 1), d(N_2)]^T$ is pre-distorted as $[x(N_1), x(N_1 + 1), x(N_1 + 2) \dots x(N_2 - 1), x(N_2)]^T$. Eq. (1) is then yielded as follows

$$\begin{cases} Ad(N_1) = Ax(N_1) + [x(N_1)^* x(N_1 + 1) + x(N_1 + 1)^* x(N_1 + 2) + \dots + x(N_2 - 1)^* x(N_2)] \\ Ad(N_1 + 1) = Ax(N_1 + 1) + [x(N_1)^* x(N_1 + 2) + x(N_1 + 1)^* x(N_1 + 3) + \dots + x(N_2 - 2)^* x(N_2)] \\ Ad(N_1 + 2) = Ax(N_1 + 2) + [x(N_1)^* x(N_1 + 3) + x(N_1 + 1)^* x(N_1 + 4) + \dots + x(N_2 - 3)^* x(N_2)] \\ \dots \\ Ad(N_2 - 1) = Ax(N_2 - 1) + [x(N_1)^* x(N_2)] \\ Ad(N_2) = Ax(N_2) \end{cases} \quad (2)$$

Eq. (2) is a nonlinear equations with $N_2 - N_1 + 1$ independent variables, $[x(N_1), x(N_1 + 1), x(N_1 + 2), \dots, x(N_2 - 1), x(N_2)]^T$. Through solving nonlinear equations, the symbol pre-distortion values can be achieved. The function of symbol pre-distortion to mitigate the impact of SSBI is shown in Fig. 2. Fig. 2 (a) presents the transmitted signal. After back-to-back transmission, the received signal is affected by SSBI as shown in Fig. 2 (b). Fig. 2 (c) presents the pre-distorted signal and Fig. 2 (d) presents the desired signal without SSBI.

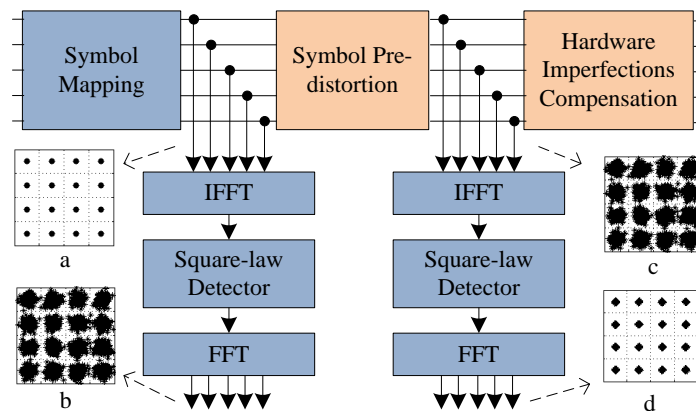


Fig 2. The function of Symbol Pre-distortion. a: Ideal constellation before Symbol Pre-distortion; b: Disturbed constellation after demodulation; c: Imperfect constellation after Symbol Pre-distortion; d: Nearly ideal constellation after demodulation

2.3. Fixed Point Iteration Solving Nonlinear Equations

To simplify the solution of solving nonlinear equations, fixed point iteration is used to approximately solve the equations. The ideal symbol mapping values are utilized as precondition. Eq. (1) shows that the rightmost subcarrier N_2 does not suffer from SSBI, so $x(N_2) = d(N_2)$. To accelerate the convergence of fixed point iteration, using the latest estimated values $x^i(1), x^i(2), \dots, x^i(k-1)$, not $x^{i-1}(1), x^{i-1}(2), \dots, x^{i-1}(k-1)$, to calculate $x^i(k)$, where i is the iteration number. This method is similar to Gauss-Seidel [11], which is used to solve the linear equations. We utilize the average value of error vector magnitude (EVM) at back-to-back transmission to evaluate the symbol pre-distortion system performance. The solid line in Fig. 3 shows the back-to-back EVM of numerical simulation versus the iteration number with different CFSR values of 8, 10, 12 and 14-dB. The CFSR is defined as $CFSR = |A|^2 / \sum |d(k)|^2$ [6], where A and $d(k)$ are the amplitude of the inserted RF-tone and the data on the k -th subcarrier respectively. Fixed point iteration is effective when CFSR is larger than 8-dB. However, even CFSR is larger than 8dB, not all of the iterations converge. Take CFSR=12-dB for example, EVM is reduced from 17.7% to 4.9% after the first iteration. However, iteration begins divergence from the second iteration which is caused by invalidation of iteration algorithm.

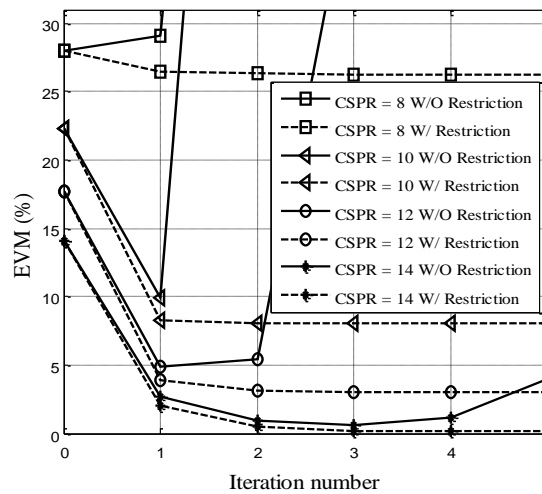


Fig 3. EVM at Back-to-back versus the iteration number at different CSPR with and without restriction

For different OFDM symbols, not all the iterations will converge. So a proper restriction to terminate iteration is necessary. The detailed process of fixed point iteration with restriction to find the optimal pre-distortion values is shown in Fig. 4. Using the i-th iteration results $[x^i(N_1), x^i(N_1+1) \dots x^i(N_2-1), x^i(N_2)]^T$ to calculate $|EVM|^i$, where $|EVM|^i$ is the average value of all data subcarriers. If $|EVM|^i$ is greater than the values of previous iteration, then terminate the iteration process. Since a large number of iterations will increase the computation complexity, a maximum iteration number should be set to balance the computation complexity and system performance. The dotted line in Fig. 3 shows the EVM with a restriction versus the iteration number at different CSPR. Take CSPR=12dB for example, EVM converges to 3.1% after 5-th iteration. The convergence of EVM values is attributed to early terminating iteration for some divergent symbols.

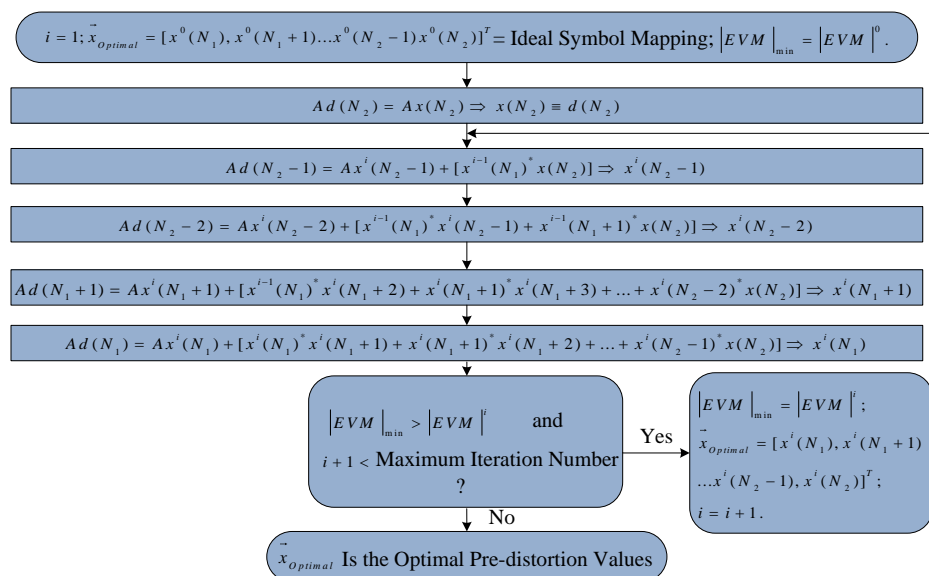


Fig 4. The process of fixed point iteration and the way to find the optimal pre-distortion values. $|EVM|^i$: Using the i-th iteration results $[x^i(N_1), x^i(N_1+1) \dots x^i(N_2-1), x^i(N_2)]^T$ to calculate the average of EVM

An advantage of fixed point iteration is lower computational complexity, but it requires a relatively higher CSPR. To the author’s best knowledge, Wu Elimination Method (WEM) [12] and Genetic Algorithms [13] have better convergence performance, but higher complexity. So developing a better-designed and lower-complexity method to solve the nonlinear equations is the key to improve the system performance.

2.4. Some Practical Implementation Issues in Symbol Pre-Distortion

In the section of theoretical models, we assume that all devices are ideal and back-to-back transmission condition. However, in practical application, signal will suffer from waveform distortions caused by frequency-dependent hardware imperfections and chromatic dispersion. In order to ensure Eq. (1) established, hardware imperfections before photo-detector and chromatic dispersion should be pre-compensated after symbol pre-distortion as shown in Fig.1.

Hardware imperfections include amplitude distortion and phase distortion. Waveform distortion compensation methods, such as frequency domain equalization (FDE) [14, 15] and time domain equalization using a finite impulse-response (FIR) filter, can be used to compensate these imperfections. FDE is more attractive in optical OFDM communication, because of the high frequency spectrum resolution and less computational complexity by only using complex multiplication before the IFFT operation.

The total length of fiber is difficult to be precisely estimated and the dispersion coefficient slowly changes with the external environment, such as temperature, so we can’t exactly estimate the total amount of dispersion. The equalization module after FFT is used to compensate the residual dispersion and waveform distortions caused by frequency-dependent hardware imperfections of receiver, especially the electric amplifiers, low-pass filter (LPF) and analog to digital converter (ADC). A specially designed training symbols with subcarrier interleaved, which can protect the training symbols from being affected by the SSBI, would be needed for channel equalization [5, 6]. The training symbols are not needed to be pre-distorted as shown in Fig. 5. The OFDM transmitted packet and the optical spectra of training symbols and data symbols are shown in Fig. 5.

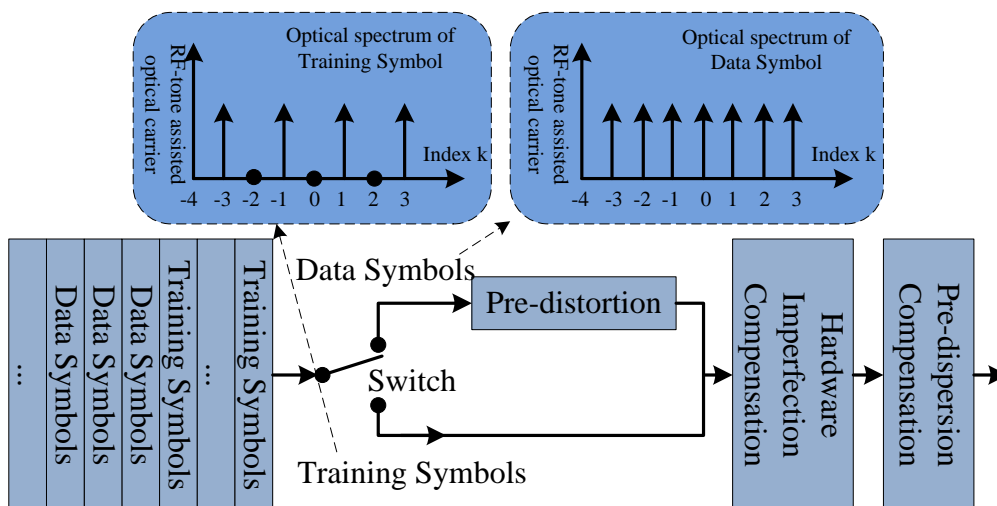


Fig 5. Optical spectra of training symbols and data symbols in a transmitted packet

3. SIMULATION AND DISCUSSION

We use MATABL and VPITransmissionMaker for simulation to assess the relative performance of the RF-tone assisted baseband optical OFDM system with and without symbol pre-distortion. The system diagram for simulation is shown in Fig. 6 and the system simulation

parameters are shown in Table 1. There are 5 different training symbols with lower peak to average power ratio (PAPR) before 400 data symbols. The raw data rate is ~40Gbps. The transfer functions of all subcarriers are obtained by the training symbol in the frequency domain. The data symbol with linear distortion, such as phase distortion caused by residual dispersion, is compensated by multiplying the inverse of transfer function.

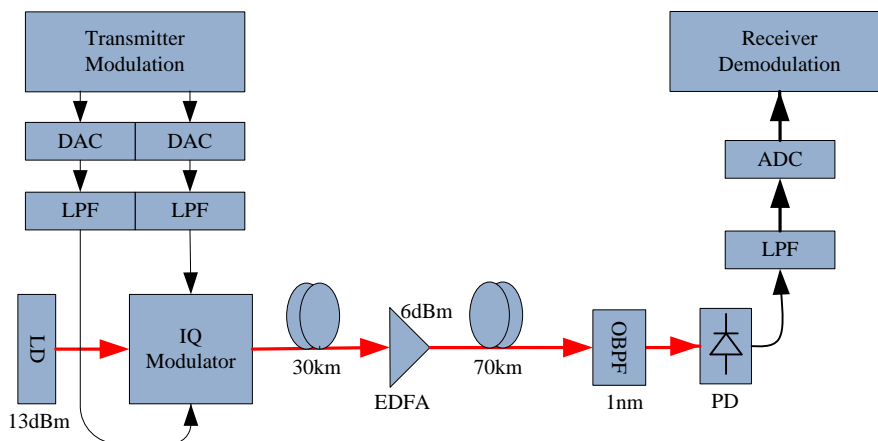


Fig 6. Simulation architecture of 40Gbps data rate

Table 1. Simulation parameters of the RF-tone assisted baseband optical OFDM system

| Parameter | Value |
|---|--|
| QAM format | 16QAM |
| IFFT and FFT size | 256, 256 |
| Number of signal subcarriers | 107 |
| Cyclic prefix | 1/8 |
| Sample rate of DAC and ADC | 24, 24GSample/s |
| Power and Line-width of laser | 13dBm, 100kHz |
| Optical modulation index [5, 6], Loss, Extinction ratio | 0.12, 5dB, 30dB |
| launch power of IQ modulator | -4dBm |
| Gain and Noise figure of EDFA | 16dB, 5dB |
| Length of SMF | 30km+70km |
| Chromatic Dispersion and Polarization Mode Dispersion | $16ps / (nm * km)$, $0.2ps / \sqrt{km}$ |
| Equivalent input noise density of PD | $1 \times 10^{-11} A / \sqrt{Hz}$ |

The system performance in terms of BER as a function of the CSNR under back-to-back condition is illustrated in Fig. 7. The maximum iteration number is set to be 8. The CSNR values of 12dB and 18dB are found to be the optimum values for the system with and without symbol pre-distortion. To the right of the optimum CSNR values with and without symbol pre-distortion, the system performance is limited by the lower photoelectric conversion efficiency [5]. To the left of the optimum CSNR=18dB without symbol pre-distortion, the system performance is limited by the SSBI, while to the left of the optimum CSNR=12dB with symbol pre-distortion, the BER deteriorate sharply with a decreasing CSNR, which is caused by the invalidation of iteration algorithm. So to further improve the receiver sensitivity of the symbol pre-distortion

system by employing a lower CSPR value [5], a better-designed and lower-complexity method of solving nonlinear equations, Eq. (2), should be developed.

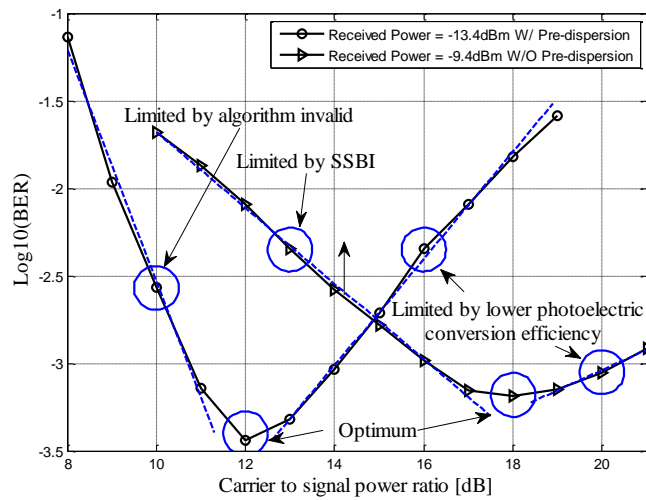


Fig 7. BER versus CSPR with and without symbol pre-distortion under back-to-back condition

The BER performance as a function of received power with and without symbol pre-distortion is shown in Fig. 8. To optimize system performance, the CSPR with pre-distortion is set to 12dB and 18dB is applied for that without pre-distortion, and other parameters are identical. The receiver sensitivity with symbol pre-distortion at forward error correction (FEC) threshold ($BER=1 \times 10^{-3}$ and redundancy ratio of 7% [16]) is ~ 4 dB better than the system without symbol pre-distortion. This is attributed to the symbol pre-distortion which reduces the requirement for CSPR and suppresses the SSBI. The symbol pre-distortion system after 100km SMF transmission has a 0.5dB power penalty compared with B2B transmission, which is caused by fiber nonlinearity Kerr effect instead of polarization mode dispersion.

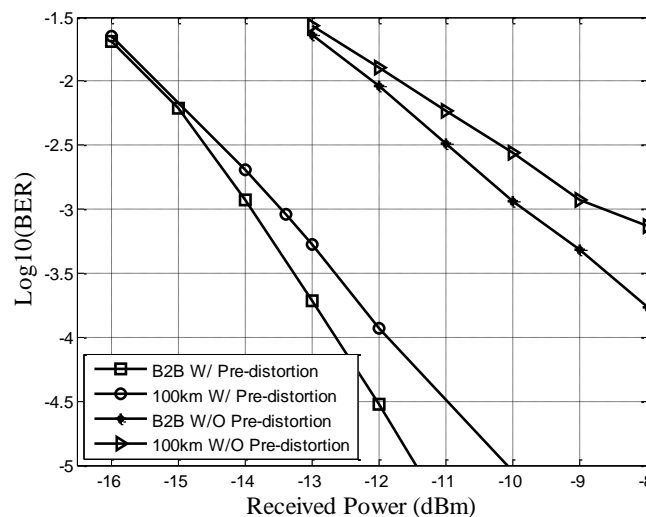


Fig 8. BER versus received power with and without symbol pre-distortion

Fig. 9 describes the received power penalty versus the residual chromatic dispersion at BER of 1×10^{-3} after 100km SMF transmission. The power penalty of 1dB tolerates residual dispersion of ~ 75 ps/nm. Therefore, the symbol pre-distortion system does not need precise

dispersion pre-compensation. This indicates that the system has the robustness towards the estimation accuracy of chromatic dispersion.

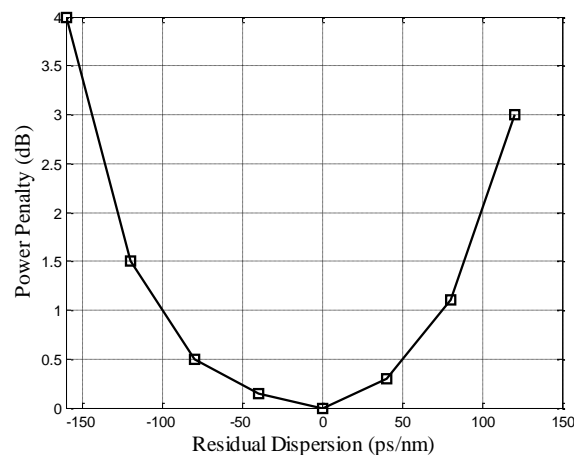


Fig 9. Received power penalty as a function of residual dispersion.

4. CONCLUSION

In conclusion, linearly field modulated, direct-detected optical OFDM suffers from SSBI, so available signal bandwidth and receiver sensitivity are seriously reduced. We propose the symbol pre-distortion method to effectively suppress the SSBI in a RF-tone assisted baseband optical OFDM system, which utilizes appropriate algorithm to solve nonlinear equations. Simulation results demonstrate that the 40Gbps 16QAM optical OFDM system based on symbol pre-distortion has a 4dB better sensitivity than that without pre-distortion after 100km SMF transmission. Therefore the symbol pre-distortion is a better method which makes lower CSRR, better receiver sensitivity and higher level modulation baseband OOFDM scheme possible.

ACKNOWLEDGEMENTS

This study is supported by National Natural Science Foundation of China (No. 61871415) and Fund of State Key Laboratory of Information Photonics and Optical Communications (Beijing University of Posts and Telecommunications), P. R. China.

REFERENCES

- [1] Chao He, Ruyan Wang, Zefu Tian, Xiang'an Tan, OFDMA-PON with MQAM downlink for flexible allocation, *Journal of Systems Engineering and Electronics*, Vol. 30 (2019) No. 6, p.1090-1095.
- [2] HALBAI F, CHEN L, PARRE S, et al. Subcarrier index power modulated optical OFDM and its performance in IMDD PON systems. *Journal of Lightwave Technology*, Vol. 34 (2016) No. 9, 2228 - 2234.
- [3] Cheng Ju, Xue Chen, Zhiguo Zhang, 40Gbps 100-km SSMF VSB-IMDD OFDM Transmission Experiment Based on FBG Filter, *OFC (2014)*, Paper Tu2G.6.
- [4] Chia-Chien Wei, Small-signal analysis of OOFDM signal transmission with directly modulated laser and direct detection, *Opt. Lett.*, 36, (2011) 151-153.
- [5] LIU Y, YANG C C, LI H B. Cost-effective and spectrally efficient coherent TDM-OFDM-PON aided by blind ICI suppression. *IEEE Photonics Technology Letters*, Vol.27 (2015) No.8, p. 887 - 890.
- [6] CVIJETIC N, QIAN D, HU J. 100 Gb/s optical access based on optical orthogonal frequency-division multiplexing. *IEEE Communications Magazine*, Vol. 48 (2010), No. 7, 70 - 77.

- [7] GUO C J, LIANG J W, LI R. Long-reach SSB-OFDM-PON employing fractional sampling and super-nyquist image induced aliasing. *Journal of Optical Communications and Networking*, Vol. 12 (2015), No. 7, p.1120 - 1125.
- [8] AMIRALIZADEH S, NGUYEN A T, PARK C S, et al. Singlefiber lightwave centralized WDM-OFDMA-PON with colorless optical network units. *Journal of Optical Communications and Networking*, Vol. 8 (2016), No. 4, 196 - 205.
- [9] Zizheng Cao, Jianjun Yu, Minmin Xia, Qi Tang, Yang Gao, Wenpei Wang, Lin Chen, Reduction of Intersubcarrier Interference and Frequency-Selective Fading in OFDM-ROF Systems, *J. Lightw. Technol.*, Vol. 28 (2010), p. 2423-2429.
- [10] Xin Wang, Jianjun Yu, Zizheng Cao, J. Xiao, Lin Chen, SSBI mitigation at 60GHz OFDM-ROF system based on optimization of training sequence, *Opt. Exp.*, Vol. 19 (2011), p. 8839-8846.
- [11] R L Burden, J D Faires, *Numerical Analysis (9th Edition)*, Michelle Julet, Boston, 2011.
- [12] Wu T, *Mathematics Mechanization*, Science Press/Kluwer Pub, chapter 3, 2000.
- [13] LI C, HU R, LI H B, et al. Digital OFDM-PON based on deltasigma modulation employing binary IM-DD channels. *IEEE Photonics Journal*, Vol. 9 (2016), No.2, 1 - 7.
- [14] Yuki Koizumi, Kazushi Toyoda, Tatsunori Omiya, Masato Yoshida, Toshihiko Hirooka, Masataka Nakazawa, 512 QAM transmission over 240 km using frequency-domain equalization in a digital coherent receiver, *Opt. Exp.*, Vol. 20 (2012) 23383-23389.
- [15] Yuki Koizumi, Kazushi Toyoda, Masato Yoshida, Masataka Nakazawa, 1024QAM (60 Gbit/s) single-carrier coherent optical transmission over 150 km, *Opt. Exp.*, Vol. 20 (2012) 12508-12514.
- [16] ITU-T Recommendation G.975.1, Appendix I.7, 2004.